Original article

Rhamnocitrin decreases fibrosis of ovarian granulosa cells by regulating the activation of the PPARγ/NF-κB/TGF-β1/Smad2/3 signaling pathway mediated by Wisp2

Yan-Yuan Zhou[1,2], Chun-Hua He[3], Huan Lan[1], Zhe-Wen Dong[1], Ya-Qi Wu[1], Jia-Le Song[4]

[1]Department of Analytical Chemistry and Drug Analysis, College of Pharmacology, Guilin Medical University, Guilin, China; [2]Guangxi Key Laboratory of Diabetic Systems Medicine, Guilin Medical University, Guilin, China; [3]Guangxi Xianzhu Traditional Chinese Medicine Technology Co. Ltd., Nanning, China; [4]Department of Nutrition and Food Hygiene, College of Public Health, Guilin Medical University, Guilin, China

Contributions: (I) Conception and design: YY Zhou; (II) Administrative support: YY Zhou; (III) Provision of study materials or patients: YY Zhou, CH He, ZW Dong; (IV) Collection and assembly of data: YY Zhou, H Lan, YQ Wu; (V) Data analysis and interpretation: YY Zhou, JL Song, YQ Wu; (VI) Manuscript writing: All authors; (VII) Final approval of manuscript: All authors.

Correspondence to: Jia-Le Song. Department of Nutrition and Food Hygiene, College of Public Health, Guilin Medical University, 1 Zhiyuan Road, Lingui District, Guilin, China. Email: songjiale@glmc.edu.cn.

Background: Polycystic ovary syndrome (PCOS) is the most common cause of anovulatory infertility in women. Rhamnocitrin (Rha) has anti-inflammatory and antioxidant actions. The WNT1-inducible-signaling pathway protein 2 (Wisp2) and nuclear factor (NF)-κB are involved in fibrosis in many diseases. We aimed to elucidate the role of Rha in fibrosis of PCOS and the underlying mechanisms.

Methods: Dehydroepiandrosterone (DHEA)-incubated ovarian granulosa KGN cells were treated by Rha. Cell proliferation was detected with cell counting kit-8 (CCK-8) and 5-ethynyul-2'-deoxyuridine (EdU) staining. The levels of Wisp2 and transforming growth factor-β1 (TGF-β1) in supernatant were measured by enzyme-linked immunosorbent assay (ELISA). We observed α-smooth muscle actin (α-SMA) protein by immunofluorescence (IF). The levels of fibrosis factors were determined using Western blot. We observed p65 nuclear translocation with confocal microscopy. We used Wisp2 overexpression and knockdown in cells treated with DHEA or Rha to validate Wisp2 function. Interaction between Wisp2 and NF-κB, as well as Wisp2 and PPARγ, were assessed by co-immunoprecipitation assay, luciferase reporter assay and chromatin immunoprecipitation (ChIP).

Results: The results showed that Rha elevated the reduced proliferation of DHEA-treated cells. In addition, Rha reversed the decreased Wisp2 and the increased TGF-β1 in supernatant. The proteins CTGF, α-SMA, Collagen I, TGF-β1, p-Smad2, and p-Smad3 were up-regulated while Wisp2, Sirt1, and PPARγ were down-regulated by DHEA treatment, which were reversed by Rha. Meanwhile, DHEA up-regulated p-IKBa and p-p65 and promoted p65 nuclear translocation, which were inhibited by Rha. These effects of Rha were antagonized by Wisp2 knockdown and were mimicked by Wisp2 overexpression. We confirmed the protein interaction between Wisp2 and NF-κB, along with Wisp2 and PPARγ.

Conclusions: Wisp2-mediated PPARγ/NF-κB/TGF-β1/Smad2/3 signaling contributes to Rha-improved ovarian granulosa cells fibrosis, suggesting Rha as a novel agent for the treatment of PCOS.

Keywords: Rhamnocitrin (Rha); WNT1-inducible-signaling pathway protein 2 (Wisp2); PPARγ/nuclear factor κB (NF-κB)/TGF-β1/Smad2/3 signaling; fibrosis; polycystic ovary syndrome (PCOS)

Page 2 of 14

Zhou et al. Rhamnocitrin improves fibrosis of ovarian granulosa cells

Introduction

Polycystic ovary syndrome (PCOS) is one of the most common metabolic and endocrine disorders in women (1). Patients with PCOS are characterized by androgen excess, chronic anovulation, insulin resistance, and ovarian fibrosis (2). A thickening of the ovarian stroma and capsule are observed in PCOS due to the elevated fibrous tissue and collagen deposition (3). Therapeutic decisions in PCOS focus on counteracting and suppressing the secretion and action of androgens, ameliorating metabolic conditions, and promoting fertility (4). More considerable advancement in understanding the pathophysiology and therapy is important for the development of innovative treatments to prevent PCOS and its long-term complications.

The application of natural products, specifically flavonoids, has achieved great attention for the treatment of many human diseases, including PCOS. Some compounds are discovered to exert beneficial influence on PCOS via reducing granulosa cell oxidative stress, regulating cell apoptosis and proliferation, affecting hormonal and metabolic parameters, as well as promoting secretion of sex hormones and ameliorating hyperandrogenism, acyclicity, infertility and follicular development (5-9). Hesperidin, a member of 3'-hydroxyflavanones, has been reported to promote follicular development in 3D culture of detached preantral ovarian follicles of mice via elevating the expressions of proliferating cell nuclear antigen (PCNA) and follicle stimulating hormone receptor (FSH-R), two key genes of folliculogenesis (9). Rhamnocitrin (Rha), a natural flavonoid isolated from herbs, has antioxidant (10) and anti-inflammatory (11) actions. *Prunus padus var. seoulensis*-derived Rha is considered as a novel potent and reversible human monoamine oxidase inhibitor (12). A previous study identified that Rha, separated from *Nervilia fordii*, could be serve as an effective inhibitor of endothelial activation induced by lipopolysaccharide (LPS) stimulation (13). However, the effect of Rha on the pathophysiological alterations in ovarian granulosa cells of PCOS has yet to be unraveled.

Currently, research has shown that PCOS is accompanied by ovarian fibrosis (2,3). The proteins in CCN family have aroused intense interest in human metabolic disorders as important fibrosis regulators (14). One such member, CCN5, also known as WNT1-inducible signaling pathway protein 2 (Wisp2), is involved in regulation of fibrosis in various diseases. It is demonstrated that Wisp2 could reverse established cardiac fibrosis by inhibiting fibroblast-to-myofibroblast trans-differentiation, suppressing endothelial-mesenchymal transition (EMT) and enhancing myofibroblast apoptosis in the myocardium (15). A previous study confirmed that endogenous CCN5/Wisp2 has an anti-fibrotic effect in hypertensive heart failure induced by high-dose Ang II (16). The overexpression of CCN5/Wisp2 inhibits profibrotic phenotypes in a lung fibrosis model *in vivo* and in lung fibroblasts separated from idiopathic pulmonary fibrosis patients (17). High expression of CCN5/Wisp2 is observed in several ovarian cancer cell lines and tissues, while deletion of CCN5/Wisp2 promotes cell apoptosis while restraining cell growth and clone formation of ovarian cancer cells (18). It is important to understand how CCN5/Wisp2 regulates fibrosis, which can be beneficial for developing novel therapeutic approaches to treat metabolic diseases, including PCOS (19).

We know that CCN5/Wisp2 specifically triggers the intrinsic apoptotic pathway in myofibroblasts, which may be caused by the capability of CCN5/Wisp2 to constrain nuclear factor (NF)-κB activity (15). It has been shown that NF-κB is a rapidly inducible transcription factor, playing an extensive role in gene induction during various cellular reactions (20); NF-κB is involved in fibrosis in many diseases. Tenofovir alafenamide fumarate (TAF)/tenofovir disoproxil fumarate (TDF) inhibits progression and boosts liver fibrosis reversion partly via NF-κB signaling pathways (21). Senescent alveolar epithelial cells (AECs) accelerate the accumulation of collagen in fibroblasts via PTEN/NF-κB signaling, leading to lung fibrosis (22). Pien Tze Huang suppresses the NF-κB pathway and promotes apoptosis in hepatic stellate cells (HSCs) to improve hepatic fibrosis (23). Besides, previous studies have demonstrated that PPARγ/TGF-β1/Smad2/3 signaling modulates tissue fibrosis in various human diseases. Capsaicin inhibits transforming growth factor-β1 (TGF-β1)/Smad signaling via PPARγ activation to prevent dimethylnitrosamine-induced hepatic fibrosis (24). Saroglitazar, a dual PPAR-α/γ agonist, inhibits the TGF-β/Smad pathway to diminish renal fibrosis caused by ureteral obstruction (25). Regulating PPAR-γ can alter the activation of hepatic stellate cells through the TGF-β1/Smad pathway, thus influencing hepatic fibrogenesis (26). Importantly, TGF-β1 has been shown to regulate Smad2/3 signaling to promote fibrosis of the surrounding ovarian tissues in endometriomas (27).

In the present work, we intended to verify whether Rha treatment contributed to the regulation of granulosa cell proliferation and fibrosis and to determine the potential mechanism of the signaling pathway in PCOS disease. The findings of our research may provide new experimental evidence for further comprehension the inhibitory effect of Rha on ovarian fibrosis in PCOS and offer new potential

therapy strategy for PCOS patients. We present the following article in accordance with the MDAR reporting checklist (available at https://atm.amegroups.com/article/view/10.21037/atm-22-2496/rc).

Methods

Cell culture

We purchased KGN cells from the Cell Bank of the Chinese Academy of Science (Shanghai, China). Cells were cultured in Dulbecco's modified Eagle medium (DMEM) including 10% fetal bovine serum (FBS; Gibco, Grand Island, NY, USA) and 1% gentamicin, and incubated in a humidified atmosphere condition at 37 ℃ with 5% CO_2. Different concentrations of dehydroepiandrosterone (DHEA; 10 nM, 100 nM, 1 µM, 10 µM, and 100 µM, Sigma-Aldrich, St. Louis, MO, USA) were then treated for 48 hours. Cells were incubated with low, medium, or high doses of Rha (Rha; 1 µM, 10 µM or 100 µM; Carbosynth, UK).

Cell counting kit-8 (CCK-8) analysis

In 96-well plates (1×10^4 cells/well), cells were seeded for 24 hours. Cell viability was measured with CCK-8 assay (Beyotime Biotechnology, Nantong, Jiangsu, China). The plates were added with CCK-8 at 24, 48, and 72 hours. The absorbance at 450 nm was measured using a microplate reader, after incubation at 37 ℃. Experiments were performed in triplicate independently to obtain the mean values.

5-ethynyul-2'-deoxyuridine (EdU) assay

Cell-light EdU DNA Cell proliferation Kit (C10310-1, RiboBio, Guangzhou, Guangdong, China) was used to measure cell proliferation. After treatment, EdU was added to KGN cells for 48 hours followed by fixation with 4% paraformaldehyde and staining with Apollo Dye Solution. DAPI was utilized to stain nucleic acids. A fluorescence microscope was utilized to take images and cell EdU incorporation was assessed by Image-Pro Plus software (Media Cybernetics, Rockville, MD, USA).

Immunofluorescence

After treatments, cells were fixed at room temperature for 30 minutes in 4% paraformaldehyde followed by permeabilization with 0.3% Triton X-100. Cells were then blocked with 3% bovine serum albumin (BSA) at 25 ℃ for 30 minutes after which they were rinsed three times with phosphate-buffered saline (PBS). Cells were then incubated with antibodies against α-SMA (1:100, Abcam, Cambridge, MA, USA) and anti-p65 (1:100, Abcam) overnight at 4 ℃. Cells were treated for 2 hours at 25 ℃ with secondary antibodies after washing with PBS. Then 4',6-diamidino-2-phenylindole (DAPI) was applied to counterstain nuclei for 30 minutes at a dilution of 1:2,000 before being imaged by Olympus laser scanning confocal microscope (FV3000; Olympus, Tokyo, Japan). For confocal observation and assessment, an inverted laser scanning Axio observer microscope (LSM 710, Zeiss, Oberkochen, Germany) with an EC Plan NeoFluor ×100/1.4 numerical aperture oil-immersion objective (Zeiss) was used with helium laser exciting at 543 nm and argon laser exciting at 488 nm.

ELISA

The differential abundance of Wisp2 and TGF-β1 proteins in supernatant was validated by ELISA kits (Boster Biosciences Co., Wuhan, Hubei, China) in line with the manufacturer's instructions. We added 100 µL of enzyme conjugate and 100 µL of antibodies to the samples. After incubation for 1 hour, the plate was rinsed three times with washing buffer for 10 seconds for each time. Substrate buffer was then added for color development, followed by the addition of termination buffer. The wavelength of 450 nm was selected to determine the optical density.

Western blot

Cells were lysed with radioimmunoprecipitation assay (RIPA) lysis buffer (Beyotime) containing protease inhibitor for 0.5 hours, prior to centrifugation for 10 minutes at 4 ℃ at 10,000×g. Bicinchoninic acid (BCA) protein assay kit (Beyotime) was utilized to measure protein concentrations. After being separated by 10% sodium dodecyl sulfate polyacrylamide gel electrophoresis (SDS-PAGE), proteins were removed to polyvinylidene fluoride (PVDF) membranes. They were then blocked for 2 hours with 5% non-fat dried milk. Next, they were treated with 5% BSA containing primary antibodies overnight at 4 ℃: anti-TGF-β1 (1:500, Santa Cruz Biotechnology, Santa Cruz, CA, USA), anti-α-SMA (1:200, Sigma-Aldrich, St. Louis, MO, USA), anti-Collagen I (1:1,000, Abcam), anti-CTGF (1:500, Santa Cruz), anti-Wisp2 (1:1,000, Arigo Biolaboratories,

Taiwan, China), anti-Sirt1 (1:1,000, Santa Cruz), anti-PPARγ (1:50, Abcam), anti-p-Smad2 (1:1,000, Abcam), anti-Smad2 (1:500, Abcam), anti-p-Smad3 (1:500, Abcam), anti-Smad3 (1:200, Abcam), anti-GAPDH (1:250; Santa Cruz), anti-p65 (1:50, Santa Cruz), anti-p-p65 (1:800 Santa Cruz), anti-IKBa (1:1,000; Santa Cruz), and anti-p-IKBa (1:1,000; Santa Cruz). After washing with tris-buffered saline with Tween 20 (TBST), horseradish peroxidase (HRP)-conjugated secondary antibodies were added and incubated for 2 hours at room temperature. Signals were evaluated using an enhanced chemiluminescence (ECL) kit. The expression of GAPDH was utilized to normalize protein levels.

Co-immunoprecipitation (Co-IP)

Co-IP was carried out in lysates from cells incubated with either normal rabbit immunoglobulin G (IgG) or NF-κB antibody at 4 ℃ overnight. After that, protein-antibody complex was treated with magnetic protein A + G beads (15 µL) at 4 ℃ for 1 hour with mild rotation. They were then rinsed with Co-IP buffer three times. The proteins were then eluted with 20 µL 1× loading buffer and boiled prior to running on 15% SDS-polyacrylamide gel. After that, they were removed to nitrocellulose membranes. Finally, antibodies against Wisp2 were utilized to immunoblot NF-κB-associated Wisp2 protein.

Dual luciferase reporter assay

Wild-type PPARγ (PPARγ-WT) and mutant type PPARγ (PPARγ-MUT) plasmids were constructed by GeneChem (Shanghai, China). We transfected PPARγ-WT, PPARγ-MUT along with Wisp2 overexpression plasmid or its negative vector, and the blank-plasmid into KGN cells separately. Luciferase reporter activity was observed by dual-luciferase reporter assay Kit (Promega, Madison, WI, USA).

Chromatin immunoprecipitation (ChIP)

To assess the influence of Wisp2 overexpression on the interaction NF-κB and target genes, ChIP test was carried out with Pierce Agarose Chip Kit (EpiGentek Group, Inc., Farmingdale, NY, USA). Cells were transfected with vector or pcDNA-Wisp2 and precipitated with NF-κB antibody (Abcam). Non-precipitated genomic DNA input was amplified as an input control. Normal rabbit IgG was applied for the negative control. After purification, the concentrations of DNAs were assessed.

Cell transfection

Knockdown of Wisp2 by small interfering RNA (siRNA) and the scrambled siRNA were purchased from GeneChem Company. The empty vector (pcDNA-NC) and Wisp2-specific pcDNA overexpression vector (OE-Wisp2) were synthesized from GeneChem Company. Cells were transfected with sh-Wisp2, sh-NC, pcDNA-Wisp2, or pcDNA-NC by Lipofectamine 2000 (Thermo Fisher Scientific, Waltham, MA, USA) for 48 hours.

Quantitative real-time PCR

The Wisp2 messenger RNA (mRNA) level was analyzed with quantitative real-time (qRT-PCR). After extraction of total RNA from cells by TRIzol reagent (Thermo Fisher), the concentration and purity of RNA were assessed with a nucleic acid protein detector (Applied Biosystems, Carlsbad, CA, USA). Subsequently, RNA (1 µL) was reversely transcribed into complementary DNA (cDNA) according to the instructions of the reverse transcription kit (Thermo Fisher). The RT-PCR was performed using SYBR Green PCR Kit (Thermo Fisher) and an Applied Biosystems 7300 Real-Time PCR System (Thermo Fisher). Primer sequences of the target genes were compounded by Servicebio Biotechnology Co., Ltd. and were presented as follows: *Wisp2* forward, 5'-CAACAATTCCTGGCGTTACCT-3' and reverse, 5'-GCCCTGTATTCCGTCTCCTT-3'; *GAPDH* forward, 5'-TCTCTGCTCCTCCCTGTTC-3' and reverse, 5'-ACACC GACCTTCACCATCT-3'. Expression of the target gene was standardized to *GAPDH* gene employing the $2^{-\Delta\Delta Ct}$ method.

Statistical analysis

The statistical software GraphPad Prism 8.00 (GraphPad Software Inc., San Diego, CA, USA) was used to assess the statistical data. For comparison between two groups, Student's *t*-test was applied to evaluate the statistics, while multiple comparisons were implemented by one-or two-way analysis of variance (ANOVA) followed by Tukey's post hoc test. Statistical significance was indicated by P values <0.05.

Results

Rha restored cell proliferation in DHEA-treated KGN

The KGN cells were cultured and incubated with different doses of DHEA. Profibrotic factors, including TGF-β1,

α-SMA, and Collagen I, were considerably increased in a dose-dependent manner of DHEA in KGN cells (P<0.01 or P<0.001, *Figure 1A*). To explore the effect of Rha on PCOS, DHEA-incubated KGN cells were treated with low, medium, or high doses of Rha (L-Rha, M-Rha, or H-Rha, respectively). In KGN cells, cell viability was dose-dependently increased after treatment with L-Rha, M-Rha, or H-Rha (P<0.05, *Figure 1B*). The EdU assay data showed that DHEA treatment notably reduced KGN cell proliferation (P<0.01, *Figure 1C*). However, Rha significantly alleviated the decrease of percentage of EdU positive KGN cells treated by DHEA (P<0.05 or P<0.01, *Figure 1C*). Our results revealed that Rha reversed DHEA-induced KGN cell proliferation reduction.

Rha improved fibrosis of KGN cells incubated with DHEA

To explore the function of Rha on KGN cell fibrosis, we detected the levels of Wisp2 and TGF-β1 with ELISA. The expression of Wisp2 e was remarkably up-regulated in DHEA-stimulated cells after Rha treatment, while TGF-β1 expression was obviously down-regulated in DHEA-stimulated cells after Rha administration (P<0.01 or P<0.001, *Figure 2A*). Upon treatment with Rha, CTGF expression in KGN was dose-dependently decreased, compared to the DHEA group. Moreover, Rha down-regulated the elevated levels of TGF-β1, α-SMA, Collagen I, p-Smad2, and p-Smad3, and up-regulated the reduced levels of Wisp2, Sirt1, and PPARγ expressions induced by DHEA (P<0.01 or P<0.001, *Figure 2B,2C*). Immunofluorescence (IF) staining showed that α-SMA expression was significantly decreased after Rha administration in comparison to the DHEA group (*Figure 2D*). The data indicated that Rha ameliorated KGN cell fibrosis.

H-Rha promoted proliferation of KGN cells through upregulation of Wisp2 expression

Next, we explored the mechanism of Rha in regulating KGN cell proliferation. The DHEA-treated KGN cells were administrated with H-Rha, sh-Wisp2, or OE-Wisp2. Higher Wisp2 mRNA expression was observed after treatment with OE-Wisp2 or H-Rha in DHEA-incubated cells in comparison with the DHEA group, and sh-Wisp2 downregulated the increased Wisp2 induced by H-Rha, as examined by qRT-PCR (P<0.001, *Figure 3A*). It was revealed that H-Rha significantly up-regulated the decreased cell viability in KGN cells treated by DHEA, which was

neutralized by Wisp2 knockdown while mimicked by Wisp2 overexpression (P<0.001, *Figure 3B*). The EdU assay results showed that Wisp2 or H-Rha significantly increased the EdU incorporation in DHEA-treated KGN cells than that treated with DHEA only, and Wisp2 knockdown neutralized the effects of H-Rha on KGN cell proliferation treated with DHEA (P<0.01, *Figure 3C*). These results indicated that H-Rha improved DHEA-caused KGN cell proliferation reduction via upregulating the expression of Wisp2.

### H-Rha improved fibrosis of KGN cell through modulating Wisp2

To examine the underlying mechanism of Rha on KGN cell fibrosis, Wisp2 and TGF-β1 levels were first assessed. It was revealed that H-Rha or Wisp2 could upregulate the declined Wisp2 level and downregulate the elevated TGF-β1 level induced by DHEA; however, the effects of Rha on Wisp2 on TGF-β1 levels were reversed by inhibition of Wisp2 (P<0.001, *Figure 4A*). The increased protein expression of CTGF induced by DHEA was reduced after H-Rha or Wisp2 treatment, whereas sh-Wisp2 administration counteracted the decreased CTGF expression by H-Rha. Overexpression of Wisp2 downregulated the elevated expressions of TGF-β1, α-SMA, Collagen I, p-p65, p-IKBa, p-Smad2, and p-Smad3 in cells induced by DHEA, and upregulated the reduced Wisp2, Sirt1, and PPARγ expressions. In DHEA-incubated KGN cells, Wisp2 knockdown up-regulated the suppressed effects of Rha on TGF-β1, α-SMA, Collagen I, p-p65, p-IKBa, p-Smad2, and p-Smad3, and downregulated the promotive effects of Rha on Wisp2, Sirt1, and PPARγ levels as confirmed by Western blot (P<0.001, *Figure 4B,4C*). The IF staining revealed that α-SMA expression was significantly decreased by Wisp2 or Rha treatment compared with the DHEA group, while sh-Wisp2 elevated the decreased α-SMA after Rha treatment (*Figure 4D*). These resulted indicated that Rha alleviated KGN cell fibrosis via modulating Wisp2 expression.

The protein interaction between Wisp2, NF-κB and PPARγ

Additionally, Co-IP exhibited that Rha enhanced the interaction of Wisp2 and NF-κB in DHEA-induced KGN cells (*Figure 5A*). The ChIP-qPCR data revealed that Wisp2 overexpression reduced the binding of NF-κB and target genes (*Figure 5B*). Dual-fluorescence immunohistochemistry and confocal analysis showed DHEA-induced p65
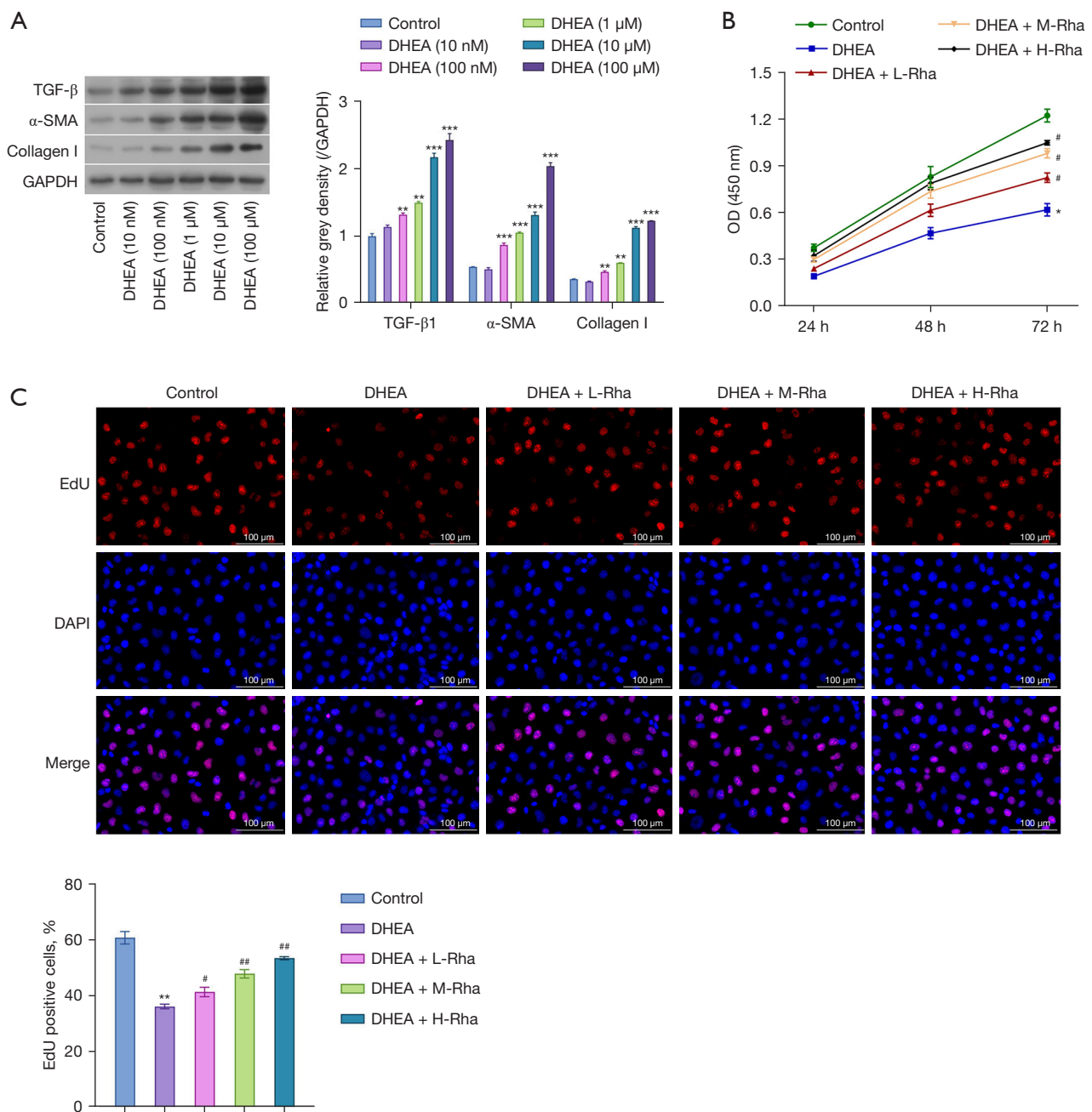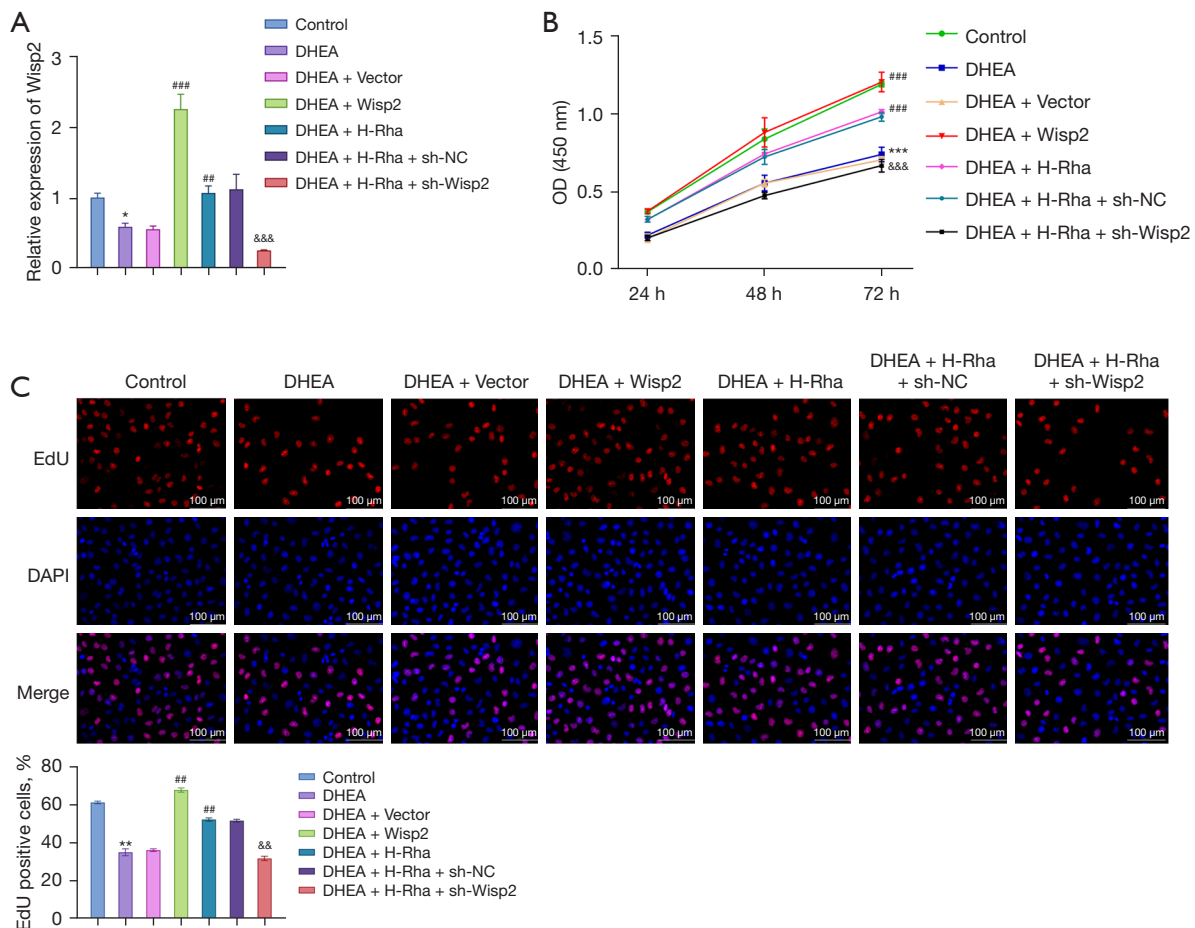
Figure 1 Rha restored cell proliferation of DHEA-treated KGN cells. (A) TGF-β1, α-SMA, and Collagen I levels in KGN cells followed by treatment with DHEA at various concentrations (10 nM, 100 nM, 1 μM, 10 μM, 100 μM) assessed using Western blot. (B) Cell viability was measured with CCK-8 after DHEA and different dosage of Rha treatment. (C) KGN cell proliferation was assessed via EdU assay after DHEA and different dosage of Rha treatment. n=3. Data are exhibited as mean ± SD. *P<0.05, **P<0.01, ***P<0.001 *vs.* control group; #P<0.05, ##P<0.01 *vs.* DHEA group. TGF-β1, transforming growth factor-β1; DHEA, dehydroepiandrosterone; CCK-8, cell counting kit-8; EdU, 5-ethynyul-2'-deoxyuridine; SD, standard deviation; OD, optical density.

Ann Transl Med 2022;10(14):789 | https://dx.doi.org/10.21037/atm-22-2496
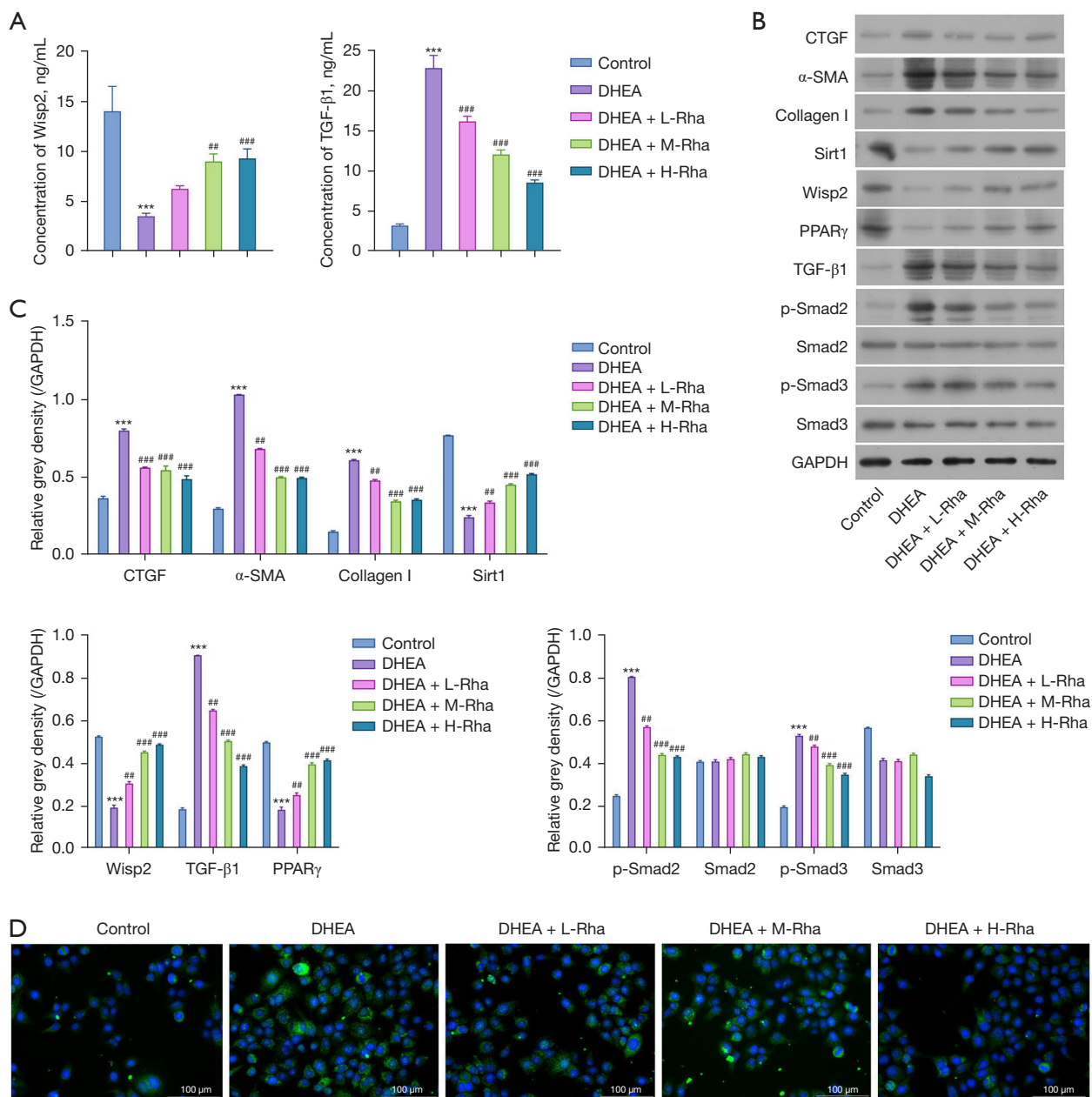
Figure 2 Rha regulated the fibrosis of KGN cells. Following DHEA and different dosage of Rha treatment, (A) Wisp2 and TGF-β1 expressions validated by ELISA; (B,C) the expressions of CTGF, TGF-β1, α-SMA, Collagen I, Sirt1, Wisp2, PPARγ, p-Smad2, Smad2, p-Smad3 and Smad3 were analyzed by Western blot. (D) α-SMA level was analyzed by IF staining. n=3. Data are exhibited as mean ± SD. ***P<0.001 *vs.* control group; ##P<0.01, ###P<0.001 *vs.* DHEA group. ELISA, enzyme-linked immunosorbent assay; IF, immunofluorescence; SD, standard deviation; DHEA, dehydroepiandrosterone.

nuclear translocation could be inhibited by Rha or Wisp2 overexpression, whereas knockdown of Wisp2 reversed the function of Rha (P<0.05) (*Figure 5C*). Compared to that in cells co-transfected with vector and PPARγ WT,

luciferase activity in cells co-transfected with Wisp2 overexpression plasmid and PPARγ WT was significantly higher. Besides, luciferase activity in the PPARγ MUT group was lower than that in PPARγ WT group, proved by

Page 8 of 14

Zhou et al. Rhamnocitrin improves fibrosis of ovarian granulosa cells

Figure 3 Rha regulated cell proliferation of KGN cells through modulating Wisp2 expression. KGN cells were treated by DHEA and H-Rha, along with Wisp2 or sh-Wisp2 transfection. (A) Wisp2 expression in KGN was examined by qRT-PCR; (B) KGN cell viability measured by CCK-8; (C) cell proliferation was detected by EdU incorporation assay. n=3. Data are exhibited as mean ± SD. *P<0.05, **P<0.01, ***P<0.001 *vs.* control group; ##P<0.01, ###P<0.001 *vs.* DHEA group; &&P<0.01, &&&P<0.001 *vs.* DHEA + H-Rha group. qRT-PCR, quantitative real-time polymerase chain reaction; CCK-8, cell counting kit-8; EdU, 5-ethynyul-2'-deoxyuridine; SD, standard deviation; DHEA, dehydroepiandrosterone; OD, optical density.

dual-luciferase reporter assay (P<0.05, *Figure 5D*), which indicated that Wisp2 could bind to NF-κB and PPARγ in KGN cells, which participated in the modulation of nuclear translocation of NF-κB.

Discussion

As a complex endocrine disorder, PCOS can result in insulin resistance, infertility, cardiovascular problems, obesity, and other related health issues, which can be distressing for women of reproductive age (28). It is essential to optimally correct metabolic homeostasis, androgen levels, and ovulation through carrying out further exploration into the

underlying basis and treatment option of PCOS (29). In this study, which to the best of our knowledge is the first of its kind, we assessed the impacts of Rha supplementation on cell proliferation in DHEA incubated-ovarian granulosa KGN cells. We also demonstrated that Rha administration in DHEA induced-KGN cells had beneficial effects on fibrosis-related factors. We validated that Rha improved fibrosis of ovarian granulosa cells via regulating Wisp2-mediated activation of NF-κB/ TGF-β1/Smad2/3 signaling.

Previous studies have reported that Rha, as a natural flavonoid, has antioxidant (10) and anti-inflammatory (11) effects. Granulosa cells offer the oocyte growth regulators and nutrients, while the oocyte facilitates the differentiation
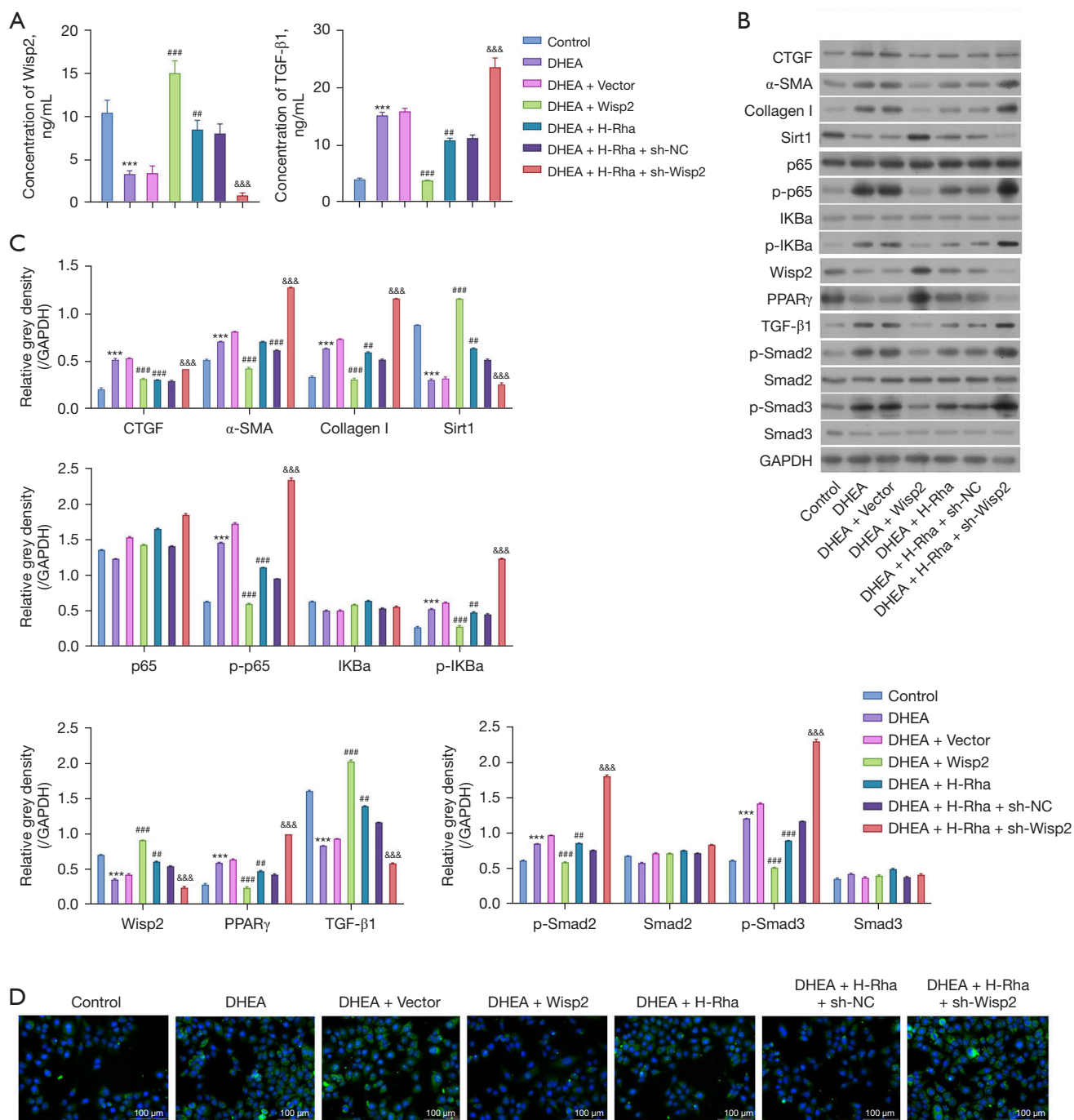
Figure 4 Rha regulated the fibrosis of KGN cells through modulating Wisp2 level. KGN cells were treated by DHEA and H-Rha, along with Wisp2 or sh-Wisp2 transfection. (A) Levels of Wisp2 and TGF-β1 were detected by ELISA. (B,C) Expressions of CTGF, TGF-β1, α-SMA, Collagen I, Sirt1, Wisp2, PPARγ, p65, p-p65, IKBa, p-IKBa, p-Smad2, Smad2, p-Smad3 and Smad3 were confirmed by Western blot. (D) α-SMA expression detected by IF staining. n=3. Data are exhibited as mean ± SD. ***P<0.001 *vs.* control group; ##P<0.01, ###P<0.001 *vs.* DHEA group; &&&P<0.001 *vs.* DHEA + H-Rha group. TGF-β1, transforming growth factor-β1; DHEA, dehydroepiandrosterone; IF, immunofluorescence; SD, standard deviation.

Page 10 of 14

Zhou et al. Rhamnocitrin improves fibrosis of ovarian granulosa cells
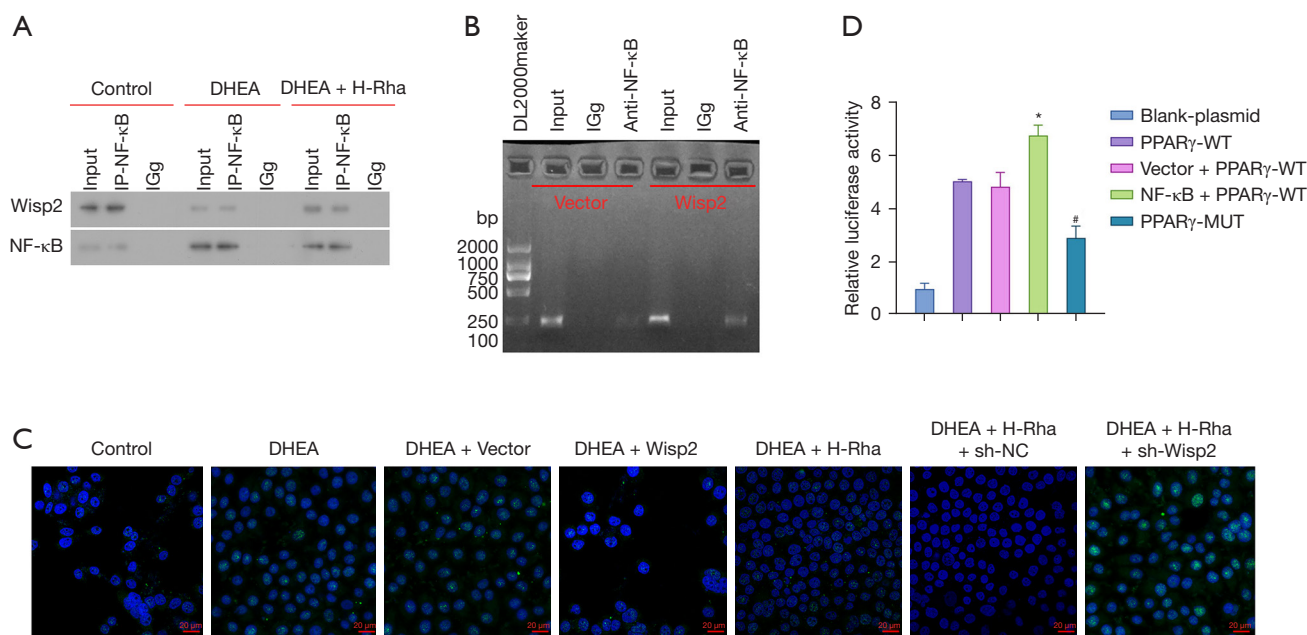
Figure 5 The interaction between Wisp2, NF-κB and PPARγ. (A) Wisp2 and NF-κB interaction was confirmed in KGN cells by Co-IP. (B) Wisp2 modulated the binding of NF-κB and downstream genes by Chip-qPCR. (C) Co-localization of p65 in KGN cells, determined by immunofluorescence detection and confocal photography. (D) Luciferase activity of KGN cells transfected with PPARγ WT, PPARγ MUT, Wisp2 overexpressed plasmid, vector, or blank plasmid, alone or in combination. n=3. Data are exhibited as mean ± SD. *P<0.05 vs. Vector + PPARγ-WT. #P<0.05 vs. Vector + PPARγ-WT and Wisp2 + PPARγ-WT. Co-IP, co-immunoprecipitation; ChIP-qPCR, chromatin immunoprecipitation polymerase chain reaction; SD, standard deviation.

and growth of granulosa cells, hence, irregular proliferation of granulosa cells may result in abnormal ovulation (30). In PCOS rats, promoting proliferation of ovarian granulosa cells can improve ovarian functions (31). In the present work, we firstly discovered that Rha supplementation effectively promoted cell viability and proliferation of ovarian granulosa KGN cells treated with DHEA. Ovarian fibrosis is observed in PCOS rats induced by androgen, which impaired ovarian functions (32). We found that fibrosis-related factors, including CTGF, TGF-β1, Collagen I, α-SMA, and p-Smad2, were up-regulated although PPARγ was down-regulated when treated with DHEA in KGN cells, and Rha reversed their expressions. In consistent with the previous literature, which reported that Rha suppressed ovarian fibrosis and lowered fibrotic factors expressions *in vivo* (33). We also demonstrated that Rha improved ovarian granulosa cell fibrosis *in vitro*. These findings provided a theoretical basis for PCOS treatment by Rha and highlighted that Rha is a potential therapeutic option for PCOS. However, further studies on pharmacokinetics and clinical trials are worthwhile.

As one of the best characterized secreted matricellular proteins of CCN family, CCN5/Wisp2 has prominent anti-fibrotic actions in various tissues, such as the heart and lungs (15-17). It is significantly elevated in several ovarian cancer cell lines and tissues (18). Serum Wisp2 levels do not change in PCOS women compared to reference individuals, while Wisp2 is associated directly with fatty acid binding protein 4 (34). We demonstrated that Rha treatment significantly increased Wisp2 expression that was dramatically reduced in DHEA-induced KGN cells. The present research is the first report to demonstrate the modulatory activity of Rha on Wisp2 in PCOS. Besides, Wisp2 knockdown antagonized those influences of Rha on cell proliferation and the expressions of fibrosis related factors, including CTGF, TGF-β1, Collagen I, α-SMA, p-Smad2, and PPARγ in DHEA treated-KGN cells. Whereas Wisp2 overexpression mimicked those effects of Rha. These findings indicates that Rha promotes cell proliferation and represses fibrosis in PCOS at least via elevating Wisp2 expression.

Total flavonoids from *Choerospondias axillaris* modulate

NF-κB signaling to diminish myocardial interstitial fibrosis (35). Morin, a member of the flavonoid family, has therapeutic potential against liver fibrosis in rats at least partly via modulation of NF-κB (36). Until now, there is no any literature could be searched concerning the modulation of Rha on NF-κB signaling. In our research, we found that Rha inhibited p-IKBa and NF-κB p-p65 expressions and the p65 nuclear translocation in DHEA-incubated ovarian granulosa cells. These inhibitory impacts of Rha on expressions of p-IKBa and p-p65 and the p65 nuclear translocation were antagonized by Wisp2 knockdown and were mimicked by Wisp2 overexpression. These discoveries are in consistence with the earlier research that CCN5/Wisp2 inhibits the activity of NF-κB in myofibroblasts (15). We also confirmed the protein interaction between Wisp2 and NF-κB by Co-IP. Wisp2 overexpression reduced the binding between NF-κB and DNA. Therefore, we suggest that Rha induces proliferation promotion and fibrosis inhibition indirectly, by regulating Wisp2-mediated NF-κB signaling.

PPAR is a member of the nuclear receptor transcription factor superfamily that participate in multiple genes expressions. Earlier literature reported that PPARγ can directly bind to the subunit p65/p50 of NF-κB and cause protein-protein interaction to form a transcriptional repression complex, which reduce the binding activity of NF-κB to DNA, thereby inhibiting the expression of related genes (37). Hydroxysafflor yellow A from Carthamus tinctorius activates PPARγ to mitigate hepatic fibrosis (38). Puerarin has an anti-fibrotic effect on hepatic fibrosis induced by CCl4 partially through regulating PPAR-γ expression in rats (39). In the present work, Rha reversed the downregulated PPARγ in KGN cells treated with DHEA, although Wisp2 knockdown antagonized the effect of Rha on PPARγ expression and Wisp2 overexpression mimicked the effects of Rha. We also validated the binding between Wisp2 and PPARγ by luciferase reporter assay. Therefore, the data indicated that Rha inhibited fibrosis of ovarian granulosa cells, by regulating Wisp2 mediated PPARγ/NF-κB signaling. Importantly, TGF-β1/Smad2/3 signaling is involved in tissue fibrosis in various diseases, which are modulated by NF-κB (24-26). In this study, Rha reversed the declined PPARγ and the elevated TGF-β1, p-Smad2 and p-Smad3 induced by DHEA. Wisp2 knockdown antagonized whereas Wisp2 overexpression mimicked the actions of Rha on PPARγ, TGF-β1, p-Smad2, and p-Smad3 expressions. Together, these activities of Rha lead to fibrosis alleviation in DHEA-incubated ovarian granulosa cells. Our results suggest that Rha exerts these impacts through constraining Wisp2-mediated activation of PPARγ/NF-κB/TGF-β1/Smad2/3 signaling, at least in part. It is possible that more profibrotic and antifibrotic molecules are involved in modulation of Rha on fibrosis of ovarian granulosa cells.

Follicular dysplasis is another major pathological feature of PCOS. Previous literature discovered that NF-κB/TGF-β1/Smad2/3 signaling took part in the regulation of follicular development. Li et al. (40) demonstrated that NF-κB exert key regulatory role in local inflammation of telomerase activity in granulosa cells and associated with follicular development. Moreover, Zhou et al. (41) reported that PPARγ coactivator-1 (PGC-1) α played modulatory role in primordial follicle formation of fetal and neonatal. Recent years, some traditional Chinese medicines have been discovered to join in modulation of follicular development. It is found that compounds isolated from herbal medicine play a beneficial role in follicular atresia caused by cell apoptosis, which improved follicular development (42). In the future, we will continue study the effects of Rha on follicular development in PCOS.

Conclusions

Treatment with Rha improved cell proliferation and fibrosis in ovarian granulosa cells incubated with DHEA. It was shown that while DHEA was decreased, Rha elevated the expression of Wisp2. We confirmed protein interaction between Wisp2 and NF-κB. It was verified that Wisp2 directly bind to PPARγ. Therefore, Rha regulates Wisp2-mediated activation of PPARγ/NF-κB/TGF-β1/Smad2/3 signaling to impact cell proliferation and fibrosis in ovarian granulosa cells treated with DHEA (Figure S1). This work proposes that Rha can be a novel option as a natural product for PCOS treatment, in spite of more animal and clinical research are still needed.

Acknowledgments

Page 12 of 14

Zhou et al. Rhamnocitrin improves fibrosis of ovarian granulosa cells

Program of Guangxi Province (S202110601088).

Footnote

Reporting Checklist: The authors have completed the MDAR reporting checklist. Available at https://atm.amegroups.com/article/view/10.21037/atm-22-2496/rc

Data Sharing Statement: Available at https://atm.amegroups.com/article/view/10.21037/atm-22-2496/dss

Conflicts of Interest: All authors have completed the ICMJE uniform disclosure form (available at https://atm.amegroups.com/article/view/10.21037/atm-22-2496/coif). CH is from Guangxi Xianzhu Traditional Chinese Medicine Technology Co. Ltd. The other authors have no conflicts of interest to declare.

Ethical Statement: The authors are accountable for all aspects of the work in ensuring that questions related to the accuracy or integrity of any part of the work are appropriately investigated and resolved.

Open Access Statement: This is an Open Access article distributed in accordance with the Creative Commons Attribution-NonCommercial-NoDerivs 4.0 International License (CC BY-NC-ND 4.0), which permits the non-commercial replication and distribution of the article with the strict proviso that no changes or edits are made and the original work is properly cited (including links to both the formal publication through the relevant DOI and the license). See: https://creativecommons.org/licenses/by-nc-nd/4.0/.

References

1. Escobar-Morreale HF. Polycystic ovary syndrome: definition, aetiology, diagnosis and treatment. Nat Rev Endocrinol 2018;14:270-84.
2. Wang D, Wang T, Wang R, et al. Suppression of p66Shc prevents hyperandrogenism-induced ovarian oxidative stress and fibrosis. J Transl Med 2020;18:84.
3. Takahashi N, Harada M, Hirota Y, et al. Activation of Endoplasmic Reticulum Stress in Granulosa Cells from Patients with Polycystic Ovary Syndrome Contributes to Ovarian Fibrosis. Sci Rep 2017;7:10824.
4. Azziz R. Polycystic Ovary Syndrome. Obstet Gynecol 2018;132:321-36.
5. Rashidi Z, Khosravizadeh Z, Talebi A, et al. Overview of biological effects of Quercetin on ovary. Phytother Res 2021;35:33-49.
6. Khorshidi M, Moini A, Alipoor E, et al. The effects of quercetin supplementation on metabolic and hormonal parameters as well as plasma concentration and gene expression of resistin in overweight or obese women with polycystic ovary syndrome. Phytother Res 2018;32:2282-9.
7. Peng MF, Tian S, Song YG, et al. Effects of total flavonoids from Eucommia ulmoides Oliv. leaves on polycystic ovary syndrome with insulin resistance model rats induced by letrozole combined with a high-fat diet. J Ethnopharmacol 2021;273:113947.
8. Hu T, Yuan X, Ye R, et al. Brown adipose tissue activation by rutin ameliorates polycystic ovary syndrome in rat. J Nutr Biochem 2017;47:21-8.
9. Shoorei H, Banimohammad M, Kebria MM, et al. Hesperidin improves the follicular development in 3D culture of isolated preantral ovarian follicles of mice. Exp Biol Med (Maywood) 2019;244:352-61.
10. Jiang H, Zhan WQ, Liu X, et al. Antioxidant activities of extracts and flavonoid compounds from Oxytropis falcate Bunge. Nat Prod Res 2008;22:1650-6.
11. Fang SH, Rao YK, Tzeng YM. Anti-oxidant and inflammatory mediator's growth inhibitory effects of compounds isolated from Phyllanthus urinaria. J Ethnopharmacol 2008;116:333-40.
12. Baek SC, Park MH, Ryu HW, et al. Rhamnocitrin isolated from Prunus padus var. seoulensis: A potent and selective reversible inhibitor of human monoamine oxidase A. Bioorg Chem 2019;83:317-25.
13. Lin T, Luo W, Li Z, et al. Rhamnocitrin extracted from Nervilia fordii inhibited vascular endothelial activation via miR-185/STIM-1/SOCE/NFATc3. Phytomedicine 2020;79:153350.
14. Sun C, Zhang H, Liu X. Emerging role of CCN family proteins in fibrosis. J Cell Physiol 2021;236:4195-206.
15. Jeong D, Lee MA, Li Y, et al. Matricellular Protein CCN5 Reverses Established Cardiac Fibrosis. J Am Coll Cardiol 2016;67:1556-68.
16. Huang A, Li H, Zeng C, et al. Endogenous CCN5 Participates in Angiotensin II/TGF-β1 Networking of Cardiac Fibrosis in High Angiotensin II-Induced Hypertensive Heart Failure. Front Pharmacol 2020;11:1235.
17. Zhang L, Li Y, Liang C, et al. CCN5 overexpression

inhibits profibrotic phenotypes via the PI3K/Akt signaling pathway in lung fibroblasts isolated from patients with idiopathic pulmonary fibrosis and in an in vivo model of lung fibrosis. Int J Mol Med 2014;33:478-86.

18. Shi ZQ, Chen ZY, Han Y, et al. WISP2 promotes cell proliferation via targeting ERK and YAP in ovarian cancer cells. J Ovarian Res 2020;13:85.

19. Grünberg JR, Elvin J, Paul A, et al. CCN5/WISP2 and metabolic diseases. J Cell Commun Signal 2018;12:309-18.

20. Zhang Q, Lenardo MJ, Baltimore D. 30 Years of NF-κB: A Blossoming of Relevance to Human Pathobiology. Cell 2017;168:37-57.

21. Zhao J, Han M, Zhou L, et al. TAF and TDF attenuate liver fibrosis through NS5ATP9, TGFβ1/Smad3, and NF-κB/NLRP3 inflammasome signaling pathways. Hepatol Int 2020;14:145-60.

22. Tian Y, Li H, Qiu T, et al. Loss of PTEN induces lung fibrosis via alveolar epithelial cell senescence depending on NF-κB activation. Aging Cell 2019;18:e12858.

23. Zheng H, Wang X, Zhang Y, et al. Pien-Tze-Huang ameliorates hepatic fibrosis via suppressing NF-κB pathway and promoting HSC apoptosis. J Ethnopharmacol 2019;244:111856.

24. Choi JH, Jin SW, Choi CY, et al. Capsaicin Inhibits Dimethylnitrosamine-Induced Hepatic Fibrosis by Inhibiting the TGF-β1/Smad Pathway via Peroxisome Proliferator-Activated Receptor Gamma Activation. J Agric Food Chem 2017;65:317-26.

25. Makled MN, El-Kashef DH. Saroglitazar attenuates renal fibrosis induced by unilateral ureteral obstruction via inhibiting TGF-β/Smad signaling pathway. Life Sci 2020;253:117729.

26. Ni XX, Li XY, Wang Q, et al. Regulation of peroxisome proliferator-activated receptor-gamma activity affects the hepatic stellate cell activation and the progression of NASH via TGF-β1/Smad signaling pathway. J Physiol Biochem 2021;77:35-45.

27. Shi LB, Zhou F, Zhu HY, et al. Transforming growth factor beta1 from endometriomas promotes fibrosis in surrounding ovarian tissues via Smad2/3 signaling. Biol Reprod 2017;97:873-82.

28. Patel S. Polycystic ovary syndrome (PCOS), an inflammatory, systemic, lifestyle endocrinopathy. J Steroid Biochem Mol Biol 2018;182:27-36.

29. Rosenfield RL, Ehrmann DA. The Pathogenesis of Polycystic Ovary Syndrome (PCOS): The Hypothesis of PCOS as Functional Ovarian Hyperandrogenism Revisited. Endocr Rev 2016;37:467-520.

30. Li M, Zhao H, Zhao SG, et al. The HMGA2-IMP2 Pathway Promotes Granulosa Cell Proliferation in Polycystic Ovary Syndrome. J Clin Endocrinol Metab 2019;104:1049-59.

31. Zheng Q, Li Y, Zhang D, et al. ANP promotes proliferation and inhibits apoptosis of ovarian granulosa cells by NPRA/PGRMC1/EGFR complex and improves ovary functions of PCOS rats. Cell Death Dis 2017;8:e3145.

32. Wang D, Wang W, Liang Q, et al. DHEA-induced ovarian hyperfibrosis is mediated by TGF-β signaling pathway. J Ovarian Res 2018;11:6.

33. Zhou Y, Lan H, Dong Z, et al. Rhamnocitrin ameliorates ovarian fibrosis via PPARγ/TGF-β1/Smad2/3 pathway to repair ovarian function in polycystic ovary syndrome rats. Research Square doi: https://doi.org/10.21203/rs.3.rs-675381/v1.

34. Almario RU, Karakas SE. Roles of circulating WNT-signaling proteins and WNT-inhibitors in human adiposity, insulin resistance, insulin secretion, and inflammation. Horm Metab Res 2015;47:152-7.

35. Sun B, Xia Q, Gao Z. Total Flavones of Choerospondias axillaris Attenuate Cardiac Dysfunction and Myocardial Interstitial Fibrosis by Modulating NF-κB Signaling Pathway. Cardiovasc Toxicol 2015;15:283-9.

36. Heeba GH, Mahmoud ME. Therapeutic potential of morin against liver fibrosis in rats: modulation of oxidative stress, cytokine production and nuclear factor kappa B. Environ Toxicol Pharmacol 2014;37:662-71.

37. Remels AH, Langen RC, Gosker HR, et al. PPARgamma inhibits NF-kappB-dependent transcriptional activation in skeletal muscle. Am J Physiol Endocrinol Metab 2009;297:E174-83.

38. Wang CY, Liu Q, Huang QX, et al. Activation of PPARγ is required for hydroxysafflor yellow A of Carthamus tinctorius to attenuate hepatic fibrosis induced by oxidative stress. Phytomedicine 2013;20:592-9.

39. Guo C, Xu L, He Q, et al. Anti-fibrotic effects of puerarin on CCl4-induced hepatic fibrosis in rats possibly through the regulation of PPAR-γ expression and inhibition of PI3K/Akt pathway. Food Chem Toxicol 2013;56:436-42.

40. Li Y, Li R, Ouyang N, et al. Investigating the impact of local inflammation on granulosa cells and follicular development in women with ovarian endometriosis. Fertil Steril 2019;112:882-91.

Page 14 of 14

Zhou et al. Rhamnocitrin improves fibrosis of ovarian granulosa cells

41. Zhou Z, Wan Y, Zhang Y, et al. Follicular development and expression of nuclear respiratory factor-1 and peroxisome proliferator-activated receptor γ coactivator-1 alpha in ovaries of fetal and neonatal doelings. J Anim Sci 2012;90:3752-61.

42. Cai L, Zong DK, Tong GQ, et al. Apoptotic mechanism of premature ovarian failure and rescue effect of Traditional Chinese Medicine: a review. J Tradit Chin Med 2021;41:492-8.

(English Language Editor: J. Jones)
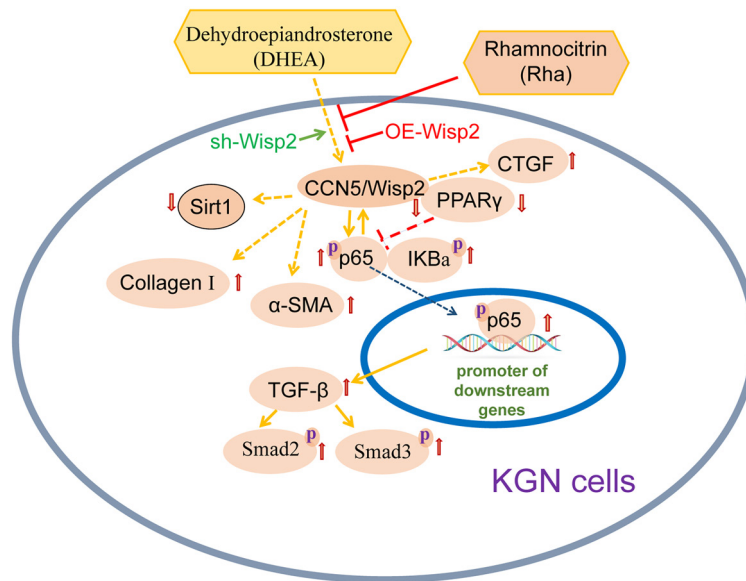
Figure S1 Graphical abstract. Dehydroepiandrosterone (DHEA) can reduce Wisp2/PPARγ expression and thereby activate NF-κB/ TGF-β1/Smad2/3 signaling pathway and elevate Collagen I, α-SMA, CTGF expression to promote fibrosis of ovarian granulosa cells. Rhamnocitrin (Rha) can improve fibrosis of ovarian granulosa cells via alleviate the influence of DHEA on Wisp2/PPARγ and downstream related-protein expression. Wisp2 overexpression (OE-Wisp2) had similar effect of Rha, while Wisp2 silence (sh-Wisp2) had opposite effect of Rha.